Diagram representations of charge pumping processes in CMOS transistors*

Huang Xinyun(黄新运)[1], Jiao Guangfan(焦广泛)[1], Shen Chen(沈忱)[2], Cao Wei(曹伟)[1], Huang Daming(黄大鸣)[1], and Li Mingfu(李名复)[1, 2, †]

(1 State Key Laboratory of ASIC & System, Department of Microelectronics, Fudan University, Shanghai 201203, China)
(2 SNDL, ECE Department, National University of Singapore, Singapore 117576, Singapore)

Abstract: A diagram representation method is proposed to interpret the complicated charge pumping (CP) processes. The fast and slow traps in CP measurement are defined. Some phenomena such as CP pulse rise/fall time dependence, frequency dependence, the voltage dependence for the fast and slow traps, and the geometric CP component are clearly illustrated at a glance by the diagram representation. For the slow trap CP measurement, there is a transition stage and a steady stage due to the asymmetry of the electron and hole capture, and the CP current is determined by the lower capturing electron or hole component. The method is used to discuss the legitimacy of the newly developed modified charge pumping method.

Key words: charge pumping; interface-trap generation; bias temperature instability; modified CP; oxide charge
DOI: 10.1088/1674-4926/31/8/084003 **PACC:** 7340Q

1. Introduction

The charge pumping (CP) technique is a well established method developed in the last century to detect interface traps in CMOS transistors[1, 2]. Recently there is renewed interest in the CP method due to the following new advancements in CMOS technology: (1) High-k gate dielectric is used to replace the conventional SiO_2 or SiON gate dielectrics with a more complicated dielectric structure with a SiO_2 interfacial layer and a high-k dielectric layer. Several works use the CP method to investigate the oxide charge distribution in high-k gate dielectrics[3−5]. (2) The interface traps generated under the bias temperature instability (BTI) stress can be recovered when the stress is interrupted[6−10], leading to underestimation of the interface trap generation rate measured by CP measurement, since the conventional CP method should interrupt the stress for more than 0.1 s during measurement[10, 11]. Recently a modified CP (MCP) method was developed to avoid the long interruption of stress during CP measurement[12, 13]. The MCP method simply extends the inversion level $V_{\rm inv}$ of the CP pulse to the stress voltage and keeps the duty cycle of $V_{\rm inv}$ as large as possible, therefore the stress is almost "on" during measurement. However, very recently, a critical concern was raised from Ref. [14] that the MCP measurement, due to the different $V_{\rm inv}$ used in the stress phase and initial/recovery phase, may measure the different CP current components contributed by the slow oxide charge (the oxide charge with long capture time constant) at the stress phase and the initial/recovery phase, causing an artificial transient jump at the beginning of the stress phase and recovery phase.

The mathematical and physical analysis of the charge pumping process is quite complicated and therefore hard to catch straightforwardly[2, 4]. In the history of physics research, the diagram method has been very powerful to illustrate and simplify complicated physical processes. A famous example is the Feynman diagram used in the perturbation theory of quantum field-electron interaction[15] to simplify the complicated high order perturbation processes in a very clear and straightforward diagram representation. In this paper, a diagram representation method is developed to illustrate at a glance the complicated CP process to catch all key points. The diagram representation is then used to analyze the CP measurement measuring interface traps and oxide charge. In particular, the method is used to demonstrate how to reduce the error due to the oxide charge contribution in the MCP method.

2. Diagram representations of CP processes

The diagrams in Fig. 1 represent the CP processes for a p-MOSFET. It illustrates all the key points in the complicated CP process in one glance. Figure 2 represents the complementary processes for an n-MOSFET. In the following, we will only discuss the case of the p-MOSFET, and the results can be extended to the n-MOSFET easily. Figure 1(a) represents one cycle of the CP pulse applied to the p-MOSFET gate. In Figs. 1(b) and 1(c), the longitudinal axes represent time t and the vertical axes represent the change of total charge ΔQ in the traps (oxide traps or interface traps) in the CP process. Figure 1(b) is for the fast trap and Figure 1(c) is for the slow trap. For the case of interface traps with uniform trap density in the energy space[2], the vertical axes also represent $E_{\rm c} - E_{\rm em}$, where $E_{\rm c}$ is the bottom of the conduction band at the surface and $E_{\rm em}$ is the quasi Fermi level of the electrons in the interface traps, as illustrated in Fig. 1(d). ΔQ curve in Fig. 1 is the simulation curve by integrating the transient CP current in Fig. 3, as will be illustrated in a later section.

Following the discussion in Ref. [2], 6 time zones are divided in Fig. 1. In zone (1), the channel surface is under accumulation and depletion and there are no holes at the channel

* Project supported by the Micro/Nano-Electronics Science and Technology Innovation Platform of Fudan University, National Natural Science Foundation of China (No. 60936005), and the National VLSI Project (No. 2009ZX02035-003).
† Corresponding author. Email: mfli@fudan.edu.cn
Received 7 January 2010, revised manuscript received 31 March 2010

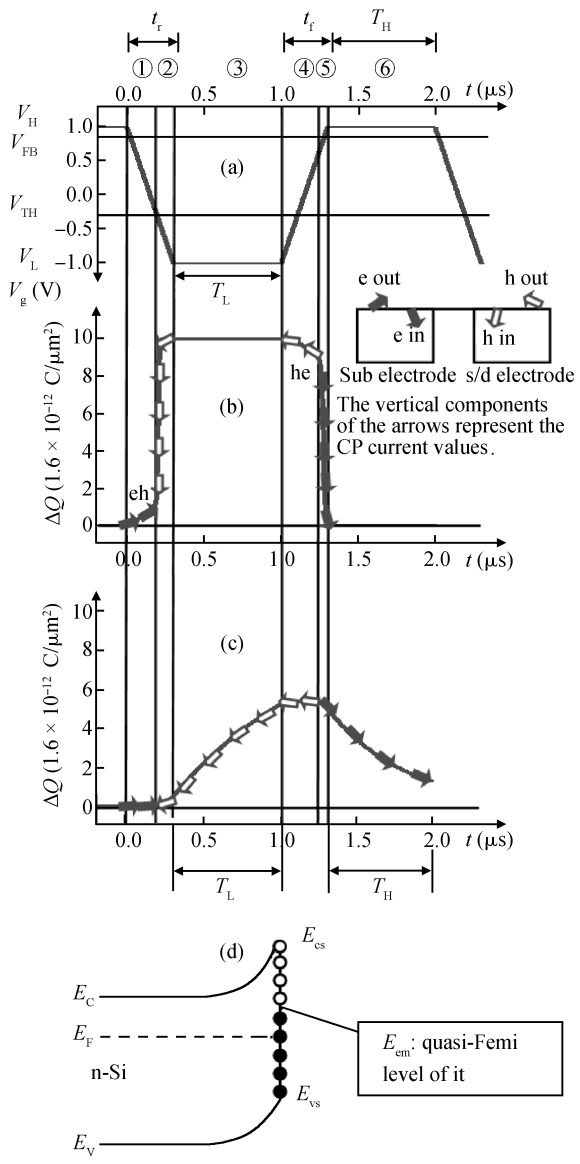

Fig. 1. (a) One CP pulse cycle applied to the p-MOSFET gate. (b) Change of charge ΔQ in the interface or fast oxide traps. The solid (open) arrows represent electron (hole) flow, corresponding to the substrate (s/d) current. The arrows oriented up represent the charge carrier (electron or holes) flow out, measured at the transistor electrode (substrate or s/d). The arrows oriented down represent the charge carrier flow into the electrode. The slope of the arrow direction represents the current value. The CP current per cycle I_{CP}/f is represented by the ΔQ difference between the eh point and the he point. Here the eh and he points are the crossing points between solid and open arrows. For more explanation see the text. (c) Same as (b) but for slow oxide traps. (d) The band diagram at the Si–SiO_2 interface. A uniform density of states of interface traps is drawn. The interface states below the quasi-Fermi energy E_{em} are all occupied by electrons while the interface states above E_{em} are all empty. E_{em} may be different from the Si bulk Fermi energy E_F in the non-steady state in the CP process[2].

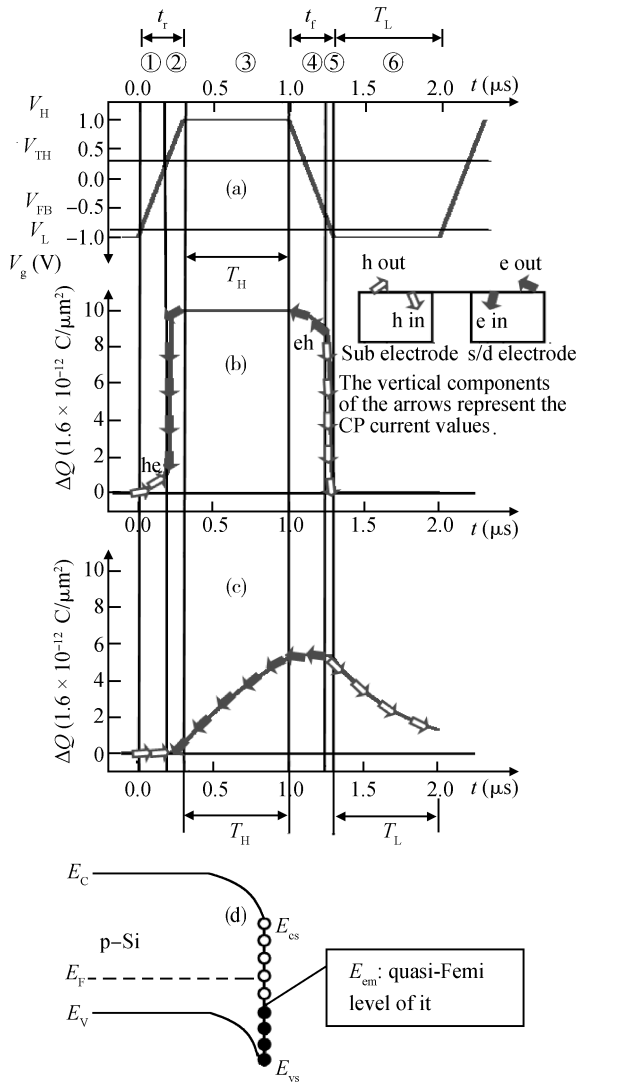

Fig. 2. Same as Fig. 1, but for an n-MOSFET. The solid (open) arrows represent electron (hole) flow, corresponding to the s/d (substrate) current. In (d), E_{em} may be different from the Si bulk Fermi energy E_F in the non-steady state in the CP process.

surface. The CP process mainly consists of electron emission from the traps to the substrate conduction band, controlled by the electron emission rate e_n, causing electrons to flow out of the substrate electrode. In zones (2) and (3, T_L), $|V_g| \geqslant |V_{TH}|$, the channel is under inversion with lots of holes. The CP process mainly consists of hole capturing by traps from the channel valence band, controlled by the hole capture time constant[2]:

$$\tau_h = \frac{1}{v_{hth}\sigma_h p_s}, \tag{1}$$

where v_{hth} is the thermal velocity of valence holes, p_s is the surface hole concentration, and σ_h is the capture cross section of hole by trap. This process causes the CP current flow into the s/d electrode. In zone (4), the surface is under inversion and depletion and there are no electrons at the channel surface. The CP process mainly consists of hole emission from the traps to the channel valence band, controlled by the hole emission rate e_h, causing CP current flow out of the s/d electrodes. In zones (5) and (6, T_H), the channel surface has a lot of electrons. The CP process mainly consists of electron capturing by traps from the substrate conduction band, controlled by electron capture time constant:

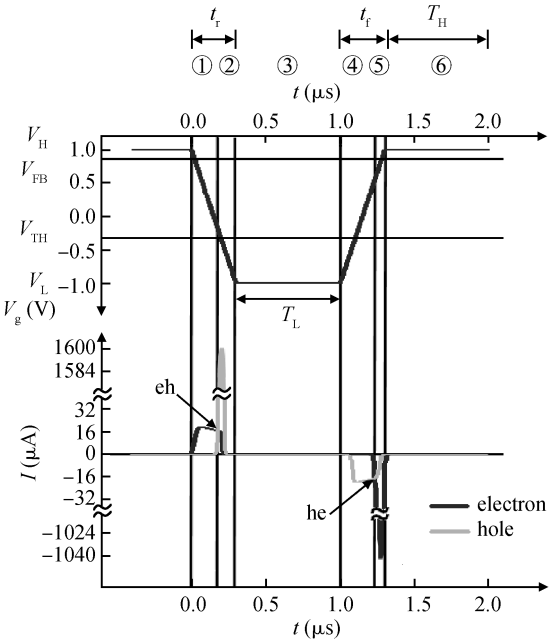

Fig. 3. Simulation results of the transient charge pumping current i in the p-MOSFET. (Two trap energy levels of 0.17 eV below the conduction band and 0.17 eV above the valance band are used. The capture cross section σ is 10^{-16} cm^2 for both electron and hole[2]. The substrate doping concentration is 5×10^{17} cm^{-3}.) The hole transient current is the simulated hole flow from the channel valence band to the interface traps. The electron transient current is the simulated electron flow from the interface traps to the substrate conduction band. There is an overlapping time region of electron emission and hole capture, close to the eh point. However, at each time instant there is a dominant process of either emission or capture, with a crossing point at eh. A similar argument is applied to the he point. The ΔQ curve in Fig. 1 corresponds to the integration curve of the transient current curve in Fig. 3.

$$\tau_e = \frac{1}{v_{eth}\sigma_e n_s}, \tag{2}$$

where v_{eth} is the thermal velocity of conduction electrons, n_s is the surface electron concentration, and σ_e is the capture cross section of electron by trap. This process causes CP current flow into the substrate electrode. The following symbols and rules are used to understand the diagram:

The solid (open) arrows represent electron (hole) flow, corresponding to the substrate (s/d) current.

The arrows oriented up represent the charge carrier (electron or holes) flow out, measured at the transistor electrode (substrate or s/d). The arrows oriented down represent the charge carrier flow into the electrode. The slope of the arrow direction represents the current value. As shown in the figure, the slope is mainly affected by τ (τ_e or τ_h). For a smaller τ value, the slope and the Q_{eh} (or Q_{he}) become larger.

The CP current per cycle I_{CP}/f is represented by the ΔQ difference between the eh (denoted byQ_{eh}) and he points (denoted by Q_{he}). Here the eh and he points are the crossing points between solid and open arrows.

$$I_{CP}/f = \Delta Q_{he} - \Delta Q_{eh}. \tag{3}$$

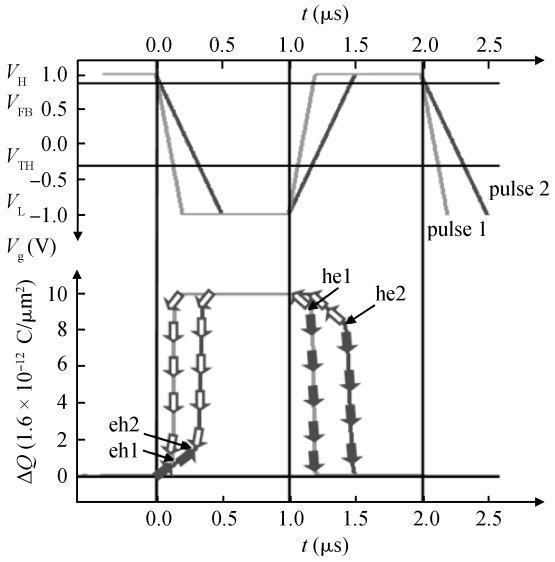

Fig. 4. According to Eq. (3) and this diagram, I_{CP}/f is reduced when the pulse rise and fall times are increased.

Figure 3 shows the numerical simulation results of the transient CP current i, using the Shockley–Read–Hall (SRH) theory of trapping dynamics[15]. The simulation was done by Silvaco Atlas software and by our own developed software with similar results. The hole transient current is the simulated hole flow from the channel valence band to the interface traps. The electron transient current is simulated electron flow from the interface traps to the substrate conduction band. From Fig. 3, there is an overlapping time region with both electron emission and hole capture processes close to the eh point. However, at each time instant there is a major process of either emission or capture. Therefore introducing the eh point which links the capture and emission arrows in Fig. 1 to simplify the process is a reasonable approximation. A similar argument is applied to the he point.

Figure 4 illustrates that the measured CP current is reduced when the pulse rise and fall times are increased[2].

3. Fast and slow traps

Both oxide traps and interface traps have the same phenomenological process in CP measurement as explained in Fig. 1. We divide all traps into two categories: (1) Fast traps with electron and hole capture time constants less than the rise and fall times of the CP pulses, and therefore ΔQ in the zones T_L and T_H are saturated as shown in the diagram representation Fig. 1(b). When the rise and fall times are in the range of 10^{-7}s ($dV/dt = 20$ V/μs in our measurements), the interface traps with capture cross section $\sigma \approx 10^{-16}$ to 10^{-15} cm^2[2] belong to the fast trap category. There is also a small amount of fast oxide traps belonging to the fast trap category with trapping/detrapping time constants shorter than 1 μs[16]. It is clear that when the dV/dt in the rise and fall time is fixed, the measured CP current per cycle I_{CP}/f contributed by the fast traps is independent of T_L and T_H (and therefore CP frequency), as shown in Fig. 5(a), and it is also independent of V_H (when V_H causes channel accumulation) and V_L (when $V_L$causes channel inversion), as shown in Fig. 6(a). (2) Slow oxide traps with electron

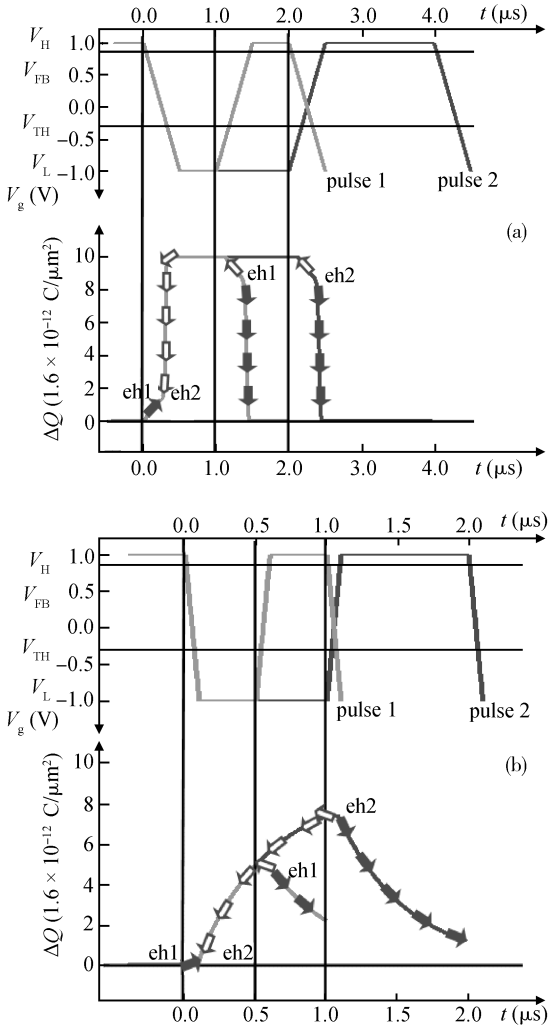

Fig. 5. According to Eq. (3) and this diagram, when dV/dt in the rise and fall time is fixed, (a) I_{CP}/f contributed by the fast traps is independent of T_L and T_H (and therefore CP frequency), (b) while that contributed by the slow oxide traps is dependent on T_L and T_H (and therefore frequency f).

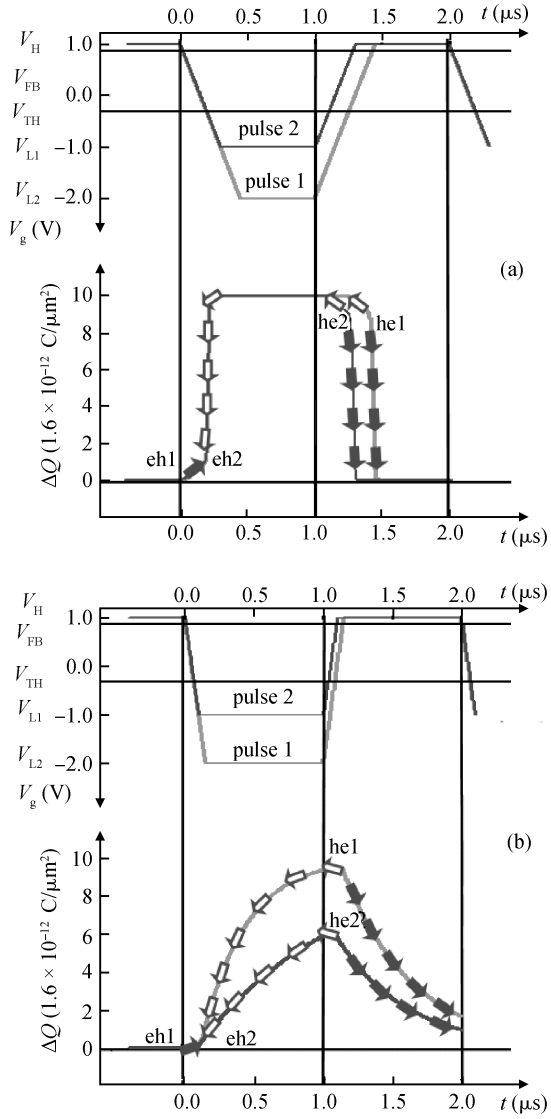

Fig. 6. According to Eq. (3) and this diagram, when the dV/dt in the rise and fall time is fixed, (a) I_{CP}/f contributed by the fast traps is independent of V_H (when V_H causes channel accumulation) and V_L (when V_L causes channel inversion), (b) while that contributed by the slow oxide traps is dependent on V_H and V_L.

and hole capture time constants longer than the rise and fall times of the CP pulse, and therefore ΔQ changes in the zones T_L and T_H as shown in the diagram in Fig. 1(c). From the diagram and Eqs. (1) and (2), it is clear that the measured I_{CP}/f contributed by the slow oxide traps is dependent on T_L and T_H (and therefore frequency f [17]), as shown in Fig. 5(b). I_{CP}/f is also dependent on V_L (or V_H) as shown in Fig. 6(b), since p_s (or n_s) in Eq. (1) (or Eq. (2)) is dependent on V_L (or V_H).

4. Analysis of the MCP measurement

The modified CP (MCP) method is a direct extension of the conventional CP method measured with the following modification to the gate pulses. (1) The low level of the gate pulse is set to be the stress voltage. (2) The duty cycle of the high level is set to a minimum, in order to reduce the recovery during the measurement[12, 13]. For the fast trap measurement, it is legitimate to use different V_L and different duty cycles in the stress phase and initial/recovery phase respectively as used in our MCP method. The number of interface traps increases under stress phase (generation) and decreases under recovery phase (recovery)[6–10]. On the other hand, as is recognized by all researchers[10, 18–20], the number of pre-existing oxide traps remains constant in both stress and recovery phases. Therefore the change of CP current ΔI_{CP} contributed by the fast traps mainly reflects the change of interface traps in the stress and recovery phases.

For the slow oxide trap measurement, one should be cautious using different V_H or V_L and different duty cycles in the stress phase and the initial/recovery phase. By using the CP diagram representation, Figure 7 illustrates the change of ΔQ in some typical CP processes used in MCP measurements. For the slow traps, ΔQ is mainly changed in T_H (substrate current) controlled by the electron capture time constant τ_e and in T_L (s/d current) controlled by the hole capture time constant τ_h. A degree of capture parameter $D = T/\tau$ is used to characterize the process, where T is T_H or T_L, while τ is τ_h or τ_e defined

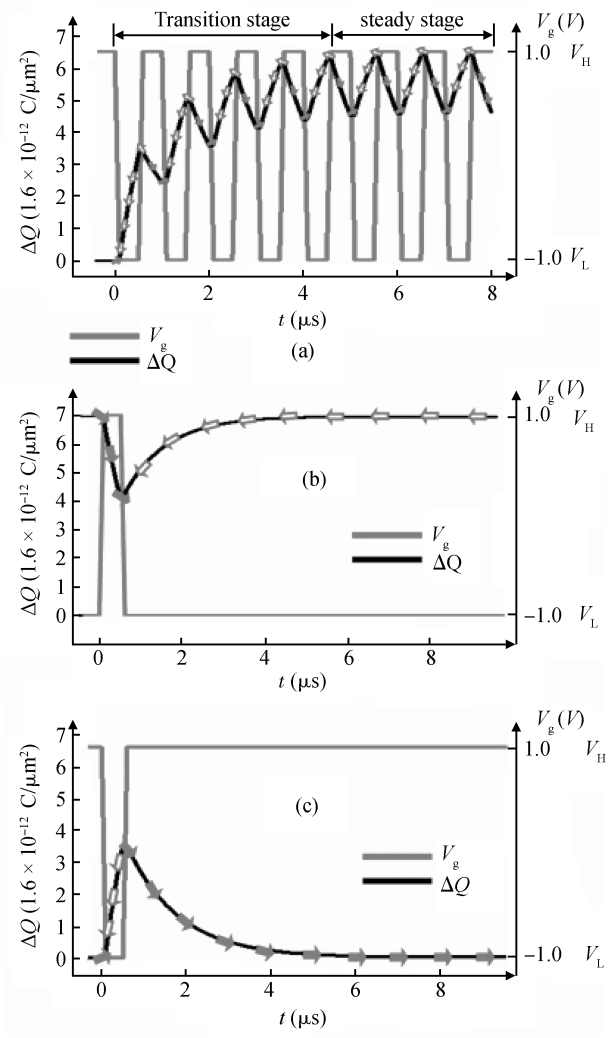

Fig. 7. Diagram representations of CP processes. (a) 50% duty cycle of the CP pulse. There is a non-steady transition stage and a steady stage. (b) A very small duty cycle of V_H is used ($T_H \ll T_L$) in the MCP measurement in the stress phase. (c) A very small duty cycle of V_L is used ($T_H \gg T_L$) in the MCP measurement in the initial/recovery phase. In all cases, reduction of either T_H or T_L can effectively suppress the CP current contributed by the slow oxide traps.

in Eqs. (1) and (2). Figure 7(a) corresponds to the case of initial/recovery measurement in the MCP method. 50% duty cycle is used with

$$\tau_e > \tau_h > T_H = T_L, \tag{4}$$

at the initial stage of $V_g = 0$ or V_{acc} before CP measurement. As shown in Fig. 7(a), there is a non-steady transition stage because $D_L = T_L/\tau_h$ in the T_L interval is larger than $D_H = T_H/\tau_e$ in the T_H interval. In this stage, $I_{s/d}$ per cycle (increase of ΔQ due to hole capturing) is larger than I_{sub} per cycle (decrease of ΔQ due to electron capturing) and there is a cumulative increase of ΔQ in one cycle. A steady stage is finally reached with $I_{sub} = I_{s/d}$ per cycle determined by the smaller D, i.e. D_H in this case. If the CP measurement time t_M (usually more than 10 ms) is much longer than τ_e and τ_h, the transition stage can be neglected.

Figure 7(b) corresponds to the case of MCP measurement in the stress phase (for the case of $\tau_e > \tau_h$). A very small duty cycle of V_H is used with $T_H \ll T_L$ and $D_H < D_L$. The CP current is determined by D_H. If the same T_H and therefore D_H is used in cases (a) and (b) in Fig. 7, both cases should measure the same I_{CP}/f contributed by the same slow oxide traps, if the transition stage in Fig. 7(a) can be neglected. For instance, case (b) using 10 kHz frequency and 1% duty cycle and case (a) using 500 kHz frequency and 50% duty cycle have the same T_H of 1 μs and therefore measure the same CP current per cycle contributed by slow oxide traps with the same τ_e. This has been verified by our experiments which will be published elsewhere.

In Fig. 7(c), a very large duty cycle of V_H is used (also for the case of $\tau_e > \tau_h$). $T_H \gg T_L$ and D_H may be larger than D_L and the CP current may be determined by D_L.

In all cases (a), (b) and (c) in Fig. 7, reduction of either T_H or T_L can effectively suppress the CP current per cycle contributed by slow traps.

As for the MCP measurement, V_L is more negative in the stress phase than in the initial/recovery phase for the p-MOSFET CP measurement[12, 13]. Therefore, for same number of interface traps, the I_{cp}/f per could be higher in the stress phase than in the initial/recovery phase due to the slow trap contribution, and might cause an abrupt change ΔI_{CP} of I_{CP} during the stress phase and initial/recovery phase transition. However, reducing either T_H or T_L in MCP can effectively suppress ΔI_{CP}. This constitutes the key guideline of the pulse design in the MCP method.

5. Experiment results and discussions

The main results obtained by the diagram representation of the CP discussed above have been demonstrated by the experimental results. The experiments were performed with p-MOSFETs with a gate width/length of 10 μm/10 μm. The gate dielectric thickness is 3.5 nm, and the nitrogen density in SiON is 4×10^{15} cm^{-2}. Figure 8(a) illustrates the V_{LOW} (the low voltage of gate pulses) dependence of the CP current (I_{CP}) measured at different $t_r = t_f$ at room temperature. During the measurements, the high voltage of gate pulses (V_{HIGH}) stays at 1.0 V. The duty cycle of gate pulses is 50% and the frequency is 10 kHz. The I_{CP} is measured from the bulk, i.e. $I_{CP} = -I_{bulk}$. As shown in Fig. 8(a), for each $t_r = t_f$, I_{CP} increases slowly when V_{LOW} decreases from –0.5 to –3.0 V. This is consistent with the results discussed in the previous section and Fig. 6. If there are only fast traps, I_{CP} is expected to be independent of V_{LOW}. However, the measured I_{CP} is the overall contribution from the fast and slow traps. The increase of I_{CP} with $-V_{LOW}$ is the contribution from slow traps. When V_{LOW} decreases, more slow traps are detected.

In addition to the V_{LOW} dependence, Figure 8(a) also shows that I_{CP} decreases when $t_r = t_f$ increases for a fixed V_{LOW}. This result has been explained in Fig. 4 and discussed in the previous section.

Figure 8(b) illustrates the V_{LOW} dependence of the CP current (I_{CP}) measured at different duty cycles (50% and 1% duty cycle respectively) at room temperature. The I_{CP} is measured from the bulk, i.e. $I_{CP} = -I_{bulk}$. For each duty cycle measurement, seven I_{CP} measurements are taken by a fixed high level of the CP pulse ($V_H = 1.0$ V), while V_L is changed from -1 to -4 V (lower curve in the hysteresis curve), and then changed

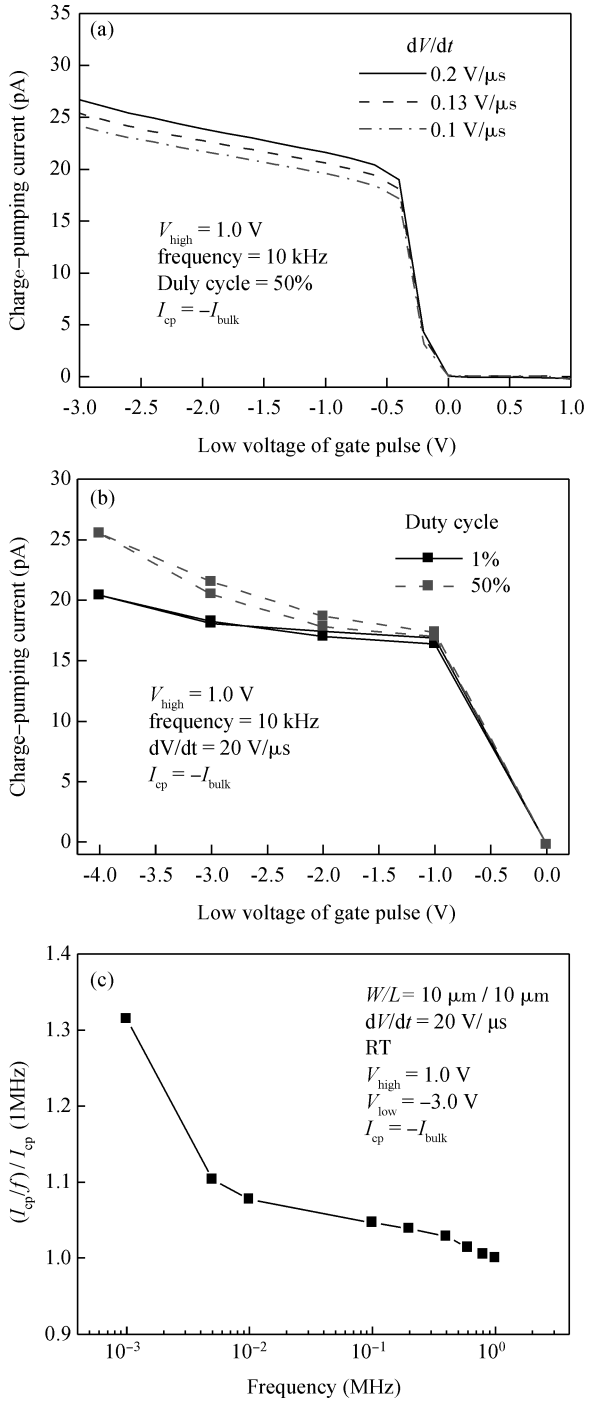

Fig. 8. (a) V_{LOW} dependence of the CP current (I_{cp}) measured at different $t_r = t_f$ at room temperature. (b) V_{LOW} dependence of the CP current (I_{cp}) measured at different duty cycles (the duty cycle is defined by $T_L/(T_L + T_H)$) at room temperature. For each duty cycle measurement, seven I_{CP} measurements are taken by a fixed high level of the CP pulse ($V_H = 1.0$ V), while V_L is changed from –1 to –4 V (lower curve in the hysteresis curve), and then changed back to –1 V (upper curve in the hysteresis curve), all with the same $dV/dt = 20$ V/μs in the rise and fall times of the pulse. (c) Normalized frequency dependence of CP current (I_{cp}) at room temperature.

back to –1 V (upper curve in the hysteresis curve), all with the same $dV/dt = 20$ V/μs in the rise and fall times of the pulse. There is an increase of I_{CP} between the lower curve and upper curve (hysteresis), reflecting the generation of new interface traps during the seven CP measurements. Comparing the curves of the 1% duty cycle with the 50% duty measurements, it is clearly shown that the 1% duty cycle overall effectively suppresses the contribution of slow oxide charge contribution in I_{CP}. It renders a weaker V_L dependence on I_{CP}.

Figure 8 (c) illustrates the normalized I_{CP}, i.e., I_{CP}/I_{CP} (1 MHz) as a function of frequency. In these measurements, V_{HIGH} is kept at 1.0 V and V_{LOW} is –3.0 V. As illustrated in the figure, I_{CP} only weakly depends on the frequency when it is higher than 10 kHz. However, I_{CP} increases more quickly for the frequency below 10 kHz. As discussed in Fig. 5, if there are only fast traps, I_{CP} is independent of the frequency. Figure 8(c) gives evidence for the coexistence of fast and slow traps since the latter contribute to a greater I_{CP} at lower frequency, consistent with Figs. 5(a) and 5(b).

The experimental results are also compared with the published literature[5, 21]. The change of I_{cp} with $-V_{LOW}$ and that of I_{CP}/f with f in our experiments are relatively small as compared with the literature because the gate dielectric of our devices is SiON with a small density of slow traps. The published results show a more pronounced change since they are from devices with high-k dielectric materials which have a higher density of oxide (slow) traps.

6. Conclusion

This paper illustrates a powerful diagram representation method to interpret the complicated charge pumping (CP) processes in MOSFETs. The fast and slow traps in CP measurement are defined. Most of the phenomena are clearly illustrated at a glance by the diagram representation. For the slow trap CP measurement, there is a transition stage and a steady stage due to the asymmetry of the electron and hole capture, and the CP current is determined by the lower electron or hole capture component. The method is used to discuss the legitimacy of the newly developed modified charge pumping (MCP) method.

References

[1] Brugler J S, Jesper P G A. Charge pumping in MOS devices. IEEE Trans Electron Devices, 1969, 16: 297

[2] Groeseneken G, Maes H, Beltran N, et al. A reliable approach to charge-pumping measurements in MOS transistors. IEEE Trans Electron Devices, 1984, 31: 42

[3] Toledano-Luque M, Degraeve R, Zahid M B, et al. New developments in charge pumping measurements on thin stacked dielectrics. IEEE Trans Electron Devices, 2008, 55: 3184

[4] Bauza D, Bayon S, Ghobar O. Further advances in the electrical characterization of silicon-insulator interface traps using charge pumping. ECS Trans, 2007, 6(3): 3

[5] Garros X, Mitard J, Leroux C, et al. In depth analysis of V_t instabilities in HfO_2 technologies by charge pumping measurements and electrical modeling. IEEE Int Reliability Physics Symp Proceedings, 2007: 61

[6] Chen G, Li M F, Ang C H, et al. Dynamic NBTI of pMOS transistors and its impact on MOSFET scaling. IEEE Electron Device Lett, 2002, 23: 734

[7] Alam M A, Mahapatra S. A comprehensive model of PMOS NBTI degradation. Microelectron Reliab, 2005, 45: 71

[8] Kaczer B, Arkhipov V, Degraeve R, et al. Disorder-controlled-kinetics model for negative bias temperature instability and its

experimental verification. Int Reliability Physics Symp Proceedings, 2005: 381

[9] Krishnan A T, Chancellor C, Chakravarthi S, et al. Material dependence of hydrogen diffusion: implications for NBTI degradation. IEDM Tech Digest, 2005: 705

[10] Yang T, Li M F, Shen C, et al. Fast and slow dynamic NBTI components in p-MOSFET with SiON dielectric and their impact on device life-time and circuit application. Symp VLSI Tech, 2005: 92

[11] Yang T, Shen C, Li M F, et al. Interface trap passivation effect in NBTI measurement for p-MOSFET with SiON gate dielectric. IEEE Electron Device Lett, 2005, 26: 758

[12] Liu W J, Liu Z Y, Huang D M, et al. On-the-fly interface trap measurement and its impact on the understanding of NBTI mechanism for p-MOSFETs with SiON gate dielectric. IEDM Tech Digest, 2007: 813

[13] Huang D M, Liu W J, Liu Z Y, et al. A modified charge pumping method for the characterization of interface traps generation in MOSFETs. IEEE Trans Electron Devices, 2009, 56: 267

[14] Hehenberger P, Aichinger T, Grasser T, et al. Do NBTI-induced interface states show fast recovery? A study using a corrected on-the-fly charge-pumping measurement technique. IEEE Int Reliability Physics Symp Proceedings 2009

[15] Li M F. Modern semiconductor quantum physics. Singapore: World Scientific, 1994

[16] Li M F, Huang D, Chen S, et al. Understanding NBTI mechanism by developing novel measurement techniques. IEEE TDMR, 2008, 8: 62

[17] Paulsen R E, White M H. Theory and application of charge pumping for the characterization of nSi-SiO_2 interface and near-interface oxide traps. IEEE Trans Electron Devices, 1994, 41: 1213

[18] Huard V, Denais M, Parthasarathy C. NBTI degradation: from physical mechanisms to modeling. Microelectron Reliab, 2006, 46: 1

[19] Grasser T, Kaczer B, Göes W, et al. A two-stage model for negative bias temperature instability. Int Reliability Physics Symp Proceedings, 2009

[20] Lee J H, Wu W H, Islam A E, et al. Separation method of hole trapping and interface trap generation and their roles in NBTI reaction-diffusion model. Int Reliability Physics Symp Proceedings, 2008: 745

[21] Rafik M, Ribes G, Ghibaudo G. Contributions and limits of charge pumping measurement for addressing trap generation in high-k/SiO_2 dielectric stacks. Int Reliability Physics Symp Proceedings, 2008: 341